Response Letter

Reviewer Comments 2

Lake ice is a very important component of the cryosphere, and couples closely with global warming and local climate. This manuscript provided a detailed method on estimating ice thickness and water level for ice-covered lakes. Some field measurements were also included to test the feasibility of the method. I think the main problems currently are the lack of some detailed explanations on method itself and also on the results, as listed below.

Response: Thanks for all these insightful and constructive comments. We have made tremendous effort to improve the clarity and consistency in the Method and Result sections and provided more discussion related to snow impact on the method as suggested by the Reviewer. Specific comments are addressed point-by-point in the following context.

1. A table summarizing all seven lakes are possible more direct to readers to understand them, except for Figure 1. And what are the red numbers in Figure 1?

Response: We have summarized related information on lakes studied in the table below. Red lines in Figure 1 represent Jason-1/2/3 ground tracks and numbers denote the track number.

Lake/region name	Mean air temperature (℃)	Winter Air temperature (℃)	Precipitation (mm)	Location	Reference
Mackenzie River basin (GBL, GSL, Athabasca Lake)	-10 – 3	-35 – -25	410	~115 °W ~62 °N	(Abdul Aziz and Burn 2006; Howell et al. 2009)
Baker Lake	-9.6	-30 – -20	157	95.28°W 64.13°N	climate.weather.gc.ca and Medeiros et al. (2012)
Winnipeg Lake	-0.7 – 1.6	-20 – -5	498	97.25°W 52.12°N	climate.weather.gc.ca and Stewardship (2011)
Hulun Lake	2.3	-16 – -10	240	117.38°E 48.97°N	(WU Qihui 2019) and (Wang et al., 2017)

Har Lake	~0.8	-15 – -5	~50	93.21°E 48.05°N	Estimated from reanalysis data

2. L147-149 can be moved to the introduction section.

Response: Done.

3. There no citation to Figure 3b. And the text on Figure 3a seems not to match the explanations on L 215-225.

Response: Figure 3b was cited in L347. We have revised Figure 3(a) to make it consistent with the method description.

4. L285ï¼Œ"the highest peak in the freezing period and the highest peak in the melting period were chosen to characterize the ice-on and ice-off dates ". It is easy to validate these dates. Do you have some validations to the field measurements? In lake ice cycle, the ice-on date and ice-off date are always not at a single day, instead the process would last for several days sometimes. But there is an obvious peak according to Figure 4, how to correspond to the real conditions in lake ice?

Response: The reviewer suggests us validating ice-on and ice-off dates identified from backscattering coefficients. The reviewer also questions how peaks in backscattering coefficients are related to real conditions in lake ice, which (based on our understanding) is characterized by events such as freeze-up start (FUS), freeze-up end (FUE), break-up start (BUS), and break-up end (BUE).

We did not find in-situ lake ice phenology data for lakes in this study, so we compared derived ice-on and ice-off dates with optical images in GSL. FUS, FUE, BUS, and BUE dates were manually identified from MODIS images from 2009 to 2016 and compared with backscatter-based ice phenology. Results shown in the figure below suggest that backscatter-based ice-on dates are very close to the FUE date (RMSE = 3 days), while backscatter-based ice-off dates are close to the BUE date (RMSE = 9 days). Given the 10-day repeat cycle of Jason-1/2/3 altimeters, the overall performance of backscatter-based ice phenology is satisfactory.

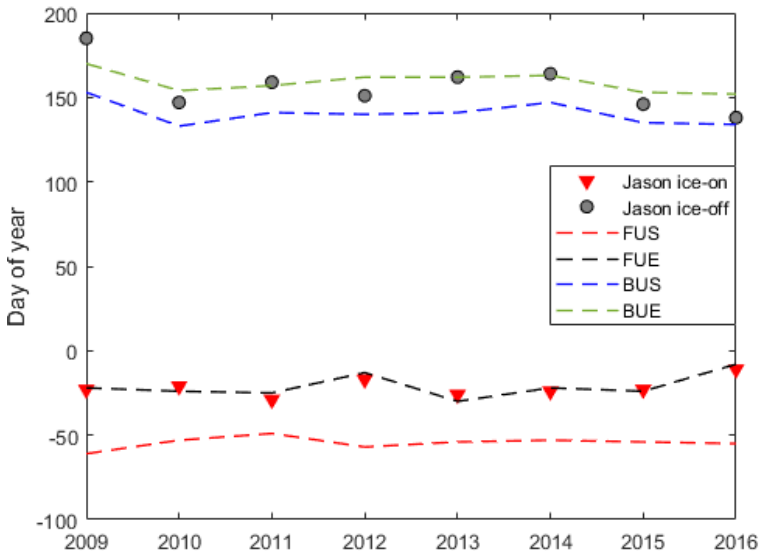

Fig R7 Comparison between the backscatter-based and the MODIS-based lake ice phenology in GSL during 2009 to 2016. FUS, FUE, BUS, and BUE denote freeze-up start, freeze-up end, break-up start, and break-up end of lake ice, respectively.

5. What is Sig on L293? Do we have a mathematical expression on function CumSum?

Response: *Sig* here represents backscattering coefficients. We have made it clear in the revised manuscript. In addition, the expression of CumSum can be written as:

$$CumSum(x_n) = \sum_{i=1}^{n} x_i$$

6. L303,"we can derive LITs based on backscattering coefficients without in situ ice thickness measurements. "I don't understand this sentence. There is not necessary to validate results of remote sensing?

Response: "we can derive LITs based on backscattering coefficients without in situ ice thickness measurements" suggests that our method can be applied to lakes without in situ data to give an initial estimation of LIT. The reason why our method does not rely on in situ information to retrieve LIT has been explained in detail in our response to Comment 35 from Reviewer 1. However, to validate the remote sensing results we still need in-situ measured LIT and snow depth as reference data.

7. L303-305. Both equation (10) and section 4.1 are cited here, then can we put these sentences in later sections?

Response: We cite Equation (10) and Section 4.1 here to help readers find core results for the application so that they do not have to go through the derivation part if not necessary.

8. The reflection on air-snow interface is not shown on Figure 5, and also not in the equation 5. A schematic diagram like Figure 5 should be placed in the front of the method section.

Response: In original Figure 5 and Equation 5, I_1 denotes the backscattered intensity from the air-snow interface and the snow-ice interface (L310). Therefore, the snow thickness was implicitly included in the derivation of the method.

However, to avoid confusion, we have used different symbols to represent the two paths in the revised manuscript as shown in the figure below. I_0 now denotes the incident intensity at the air-snow interface, I_1 denotes the backscattered intensity from the air-snow interface, I_2 denotes the backscattered intensity from the snow-ice interface, and I_3 denotes the backscattered intensity from the ice-water interface. In addition, we have moved Figure 5 to the front of the Method Section as suggested.

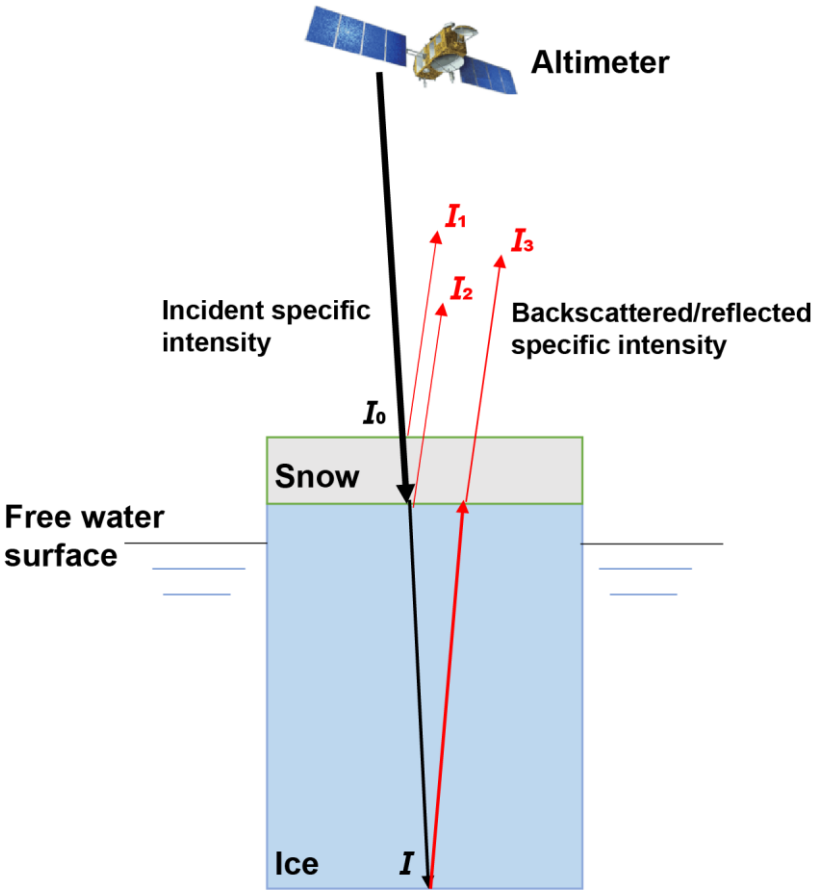

Fig R8 Modified Figure 5

9. Equation 6, Hi should be the ice thickness, not the thickness of snow and ice if according to Figure 5.

Response: We have revised this part. Now H_i denotes the lake ice thickness, and H_s denotes the lake snow depth. The revised derivation of Equations 5–11 is detailed in our response to Comment 10 of Reviewer 2.

10. In equations 5-11, there are some key points not mentioned. First, snow thickness cannot be ignored because it was even larger than the ice thickness on some boreal lakes. Secondly, main reflections occur on the air-snow interface rather than the snow-ice interface, the attenuation in the snow layer also cannot be ignored. Overall, snow is a key impact factors on the lake ice remotes sensing, do we have some discussions on this issue, especially for equations 5-11?

Response: This reviewer suggests: (1) considering the snow thickness in the derivation of Equations 5–11 and (2) providing a discussion on the reflection and attenuation of the radar pulse in snow layers.

We did not ignore lake surface snow. In fact, we have suggested in the manuscript that the backscattered intensity from the upper layer could come from the snow-air interface (L 319) and the derived backscattered-LIT and waveform-based LIT is close to the total thickness of ice and snow. To make this point clearer, we have revised this part as suggested by the reviewer. But the core results (the logarithmic regression model) did not change.

To simplify this analysis, we assumed an effective extinction coefficient *k* for both snow and ice layers. As suggested by the Reviewer, backscattering from the snow-ice interface is very small, so we used a constant to approximate the backscattered intensity from the air-snow interface and snow-ice interface**.** In the revised manuscript, Equations 5–11 are now written as:

$$I_b = I_1 + I_2 + I_3 = R_1 I_0 + I_2 + I_3 \quad (5)$$

$$I_2 = R_2(1 - R_1)I_0 \times e^{-2kH_s} \quad (6)$$

$$I_3 = R_3(1 - R_2)(1 - R_1)I_0 \times e^{-2k(H_s+H_i)} \quad (7)$$

$$I_b = (R_1 I_0 + I_2) + R_3(1 - R_2)(1 - R_1)I_0 \times e^{-2k(H_s+H_i)} \quad (8)$$

$$\sigma_0 = A + B \times e^{-K(H_s+H_i)} \quad (9)$$

$$(H_s + H_i) = -\frac{1}{K} \times \ln(\sigma_0 - A) + C, C = \frac{\ln(B)}{K} \quad (10)$$

$$\sigma_0 = A + \sigma_{max} \times e^{-K(H_s+H_i)} \quad (11)$$

where I_0, I_1, I_2, and I_3 denote the incident intensity at the air-snow interface, the backscattered intensity from the air-snow interface, the backscattered intensity from the snow-ice interface, and the backscattered intensity from the ice-water interface. As shown in revised Fig. 5., R_1, R_2, and R_3 denote the reflectance from air-snow, snow-ice, and ice-water interfaces. I_b is total backscattered intensity, H_s is the snow depth, H_i is the ice thickness, k is the effective extinction coefficient of lake ice and snow, and σ_0 is the backscattering coefficient. A, C, and K are model parameters to be calibrated.

As for the impact of snow on lake ice remote sensing, please see our response to Comment 13 of Reviewer 2.

11. There are some obvious unusual points on Figure 7a, do we have some explanations here?

Response: The outliers marked by orange circles in Figure 7(a) (shown below) are caused mostly by the initial condition of LIT and the nature of the power function model (Zakharova et al., 2021). As we mentioned earlier, the Jason-detected ice-on date is close to the FUE when thin lake ice has completely covered the lake surface. Based on the power function model, on the ice-on date detected by Jason-1/2/3, the initial backscattered LIT equals zero, but the real LIT could be several decimeters. Therefore, the outliers are located on the y-axis.

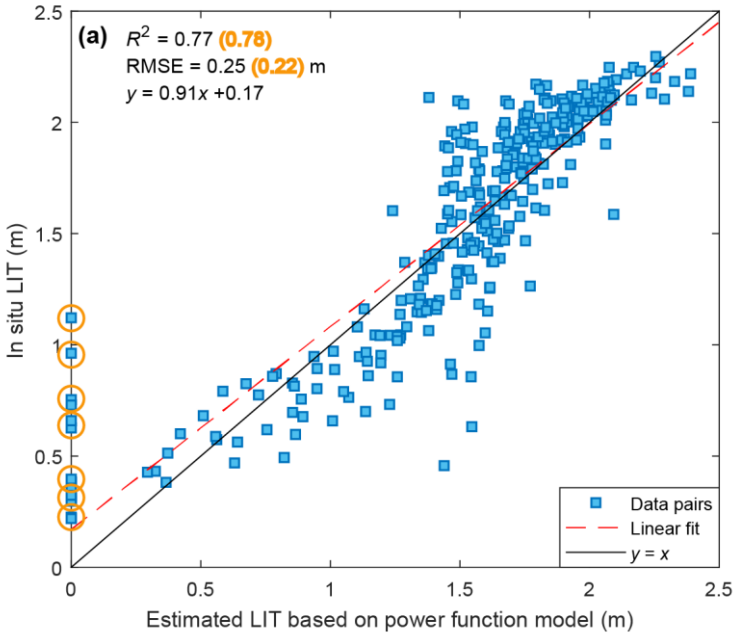

Figure 7(a) Scatter plot of in situ LIT and backscattered LIT (power function model) in GSL

12. Figures 8-9. These lakes belongs to totally different climate regions. The snow and ice thickness of Baker Lake and GSL are larger than that of Hulun Lake and Har Lake. Thicker snow will introduce more uncertainty into remote sensing as the author said on L446-448, but the results in Figure 8 seems to be better than that in Figure 9. And why CC was employed in Figure 8 while R2 was in Figure 9?

Response: We have unified the metrics in Figures 8 and 9. We also provided a table to summarize the metrics of the four lakes as shown below. The CC of Hulun Lake is 0.94, similar to Baker Lake, while the CC of Har Lake is 0.89, higher than GSL. The method has the best performance in Hulun Lake, consistent with the argument that the method is more efficient in lakes with less snow cover. As for Har lake, the lower performance is probably caused by the small cross-section of the lake as we mentioned in the manuscript (L 452).

Lake name	CC	RMSE (m)	Reference data
Baker Lake	0.94	0.24	In situ
Great Slave Lake	0.80	0.17	In situ
Hulun Lake	0.94	0.11	Modeled
Har Lake	0.89	0.20	Modeled

13. The radar backscattering coefficient depends on the ice crystal type such as granular ice and columnar ice, and also on the gas bubble size, ice salinity et al. The information on the ice physics are not mentioned here, and will the difference in ice physics of these lakes pose some impacts on the thresholding process?

Response: Ice and snow physics is very important for understanding observed microwave signals in lake ice. Several studies have discussed the lake ice and snow physics and their impacts on SAR imaging systems which has large incident angle compared to altimetry systems (Atwood et al. 2015; Gherboudj et al. 2009; Han and Lee 2012; Tjuatja et al. 1992). Here we try to provide an overall description of possible impacts of the snow and ice physics based on the literature.

Regarding backscattering coefficients, surface scattering is affected by the roughness and dielectric constant (ε) of the snow/ice surface; volume scattering is caused by snow particles and air bubbles captured inside ice, while ice-bottom scattering is controlled mostly by the roughness and ε of the ice/water interface. Snow cover can increase backscattering coefficients of Ku-band radar obtained from frozen lakes (Gunn et al. 2015). Based on Kim et al. (1984), thicker snow cover contributes more to backscattering coefficients due to enhanced volume scattering. Among the rest backscattering sources, lake ice bubbles were initially regarded as an important factor. However, Atwood et al. (2015) show that backscattering from ice bubbles is insignificant in terms of magnitude compared with reflectance from the ice-water interface. Therefore, the roughness of the ice-water interface could be a critical factor that controls the backscattered intensity.

We can conclude that backscattering coefficients obtained from thick snow-covered lakes correspond to more information from the snow layer and less information from the ice layer, contributing to larger uncertainty in these lakes. On the other hand, the roughness of the ice-water interface has a large influence on the backscattered intensity, which could be the reason why the relationship between LIT and backscattering coefficients varies considerably from year to year.

For the waveform-based LIT, the most important physical property is the ε of snow and ice, as it determines the speed of light within snow and ice and the timing of reflected

signals from different interfaces (higher ε corresponds to the lower speed of light). During the ice accumulation process, the ε of ice is relatively stable. The ε of dry snow is almost solely dependent on the snow density (Tiuri et al. 1984), which can be approximated with $\varepsilon = 1 + 2\rho$, where ρ is the relative snow density (with respect to water).

We used the same constant ε for both ice and snow, which is a compromise as we do not have any prior information related to snow depth and density. Because the waveform-based method measures the time difference between different interfaces, at the beginning of ice and snow accumulation, our method could slightly underestimate the total thickness of snow and ice because snow has a smaller ε and a larger speed of light. As the snow becomes denser during the frozen period and the speed of light becomes slower in snow, the waveform-based LIT could be closer to the total thickness of snow and ice.

References

Abdul Aziz, O.I., & Burn, D.H. (2006). Trends and variability in the hydrological regime of the Mackenzie River Basin. *Journal of Hydrology, 319*, 282-294

Atwood, D.K., Gunn, G.E., Roussi, C., Wu, J., Duguay, C., & Sarabandi, K. (2015). Microwave backscatter from Arctic lake ice and polarimetric implications. *IEEE Transactions on Geoscience and Remote Sensing, 53*, 5972-5982

Gherboudj, I., Bernier, M., & Leconte, R. (2009). A backscatter modeling for river ice: Analysis and numerical results. *IEEE Transactions on Geoscience and Remote Sensing, 48*, 1788-1798

Gunn, G.E., Brogioni, M., Duguay, C., Macelloni, G., Kasurak, A., & King, J. (2015). Observation and modeling of X-and Ku-band backscatter of snow-covered freshwater lake ice. *IEEE Journal of Selected Topics in Applied Earth Observations and Remote Sensing, 8*, 3629-3642

Han, H., & Lee, H. (2012). Radar backscattering of lake ice during freezing and thawing stages estimated by ground-based scatterometer experiment and inversion from genetic algorithm. *IEEE Transactions on Geoscience and Remote Sensing, 51*, 3089-3096

Howell, S.E.L., Brown, L.C., Kang, K.-K., & Duguay, C.R. (2009). Variability in ice phenology on Great Bear Lake and Great Slave Lake, Northwest Territories, Canada, from SeaWinds/QuikSCAT: 2000–2006. *Remote Sensing of Environment, 113*, 816-834

Kim, Y.-S., Onstott, R., & Moore, R. (1984). Effect of a snow cover on microwave backscatter from sea ice. *IEEE Journal of oceanic Engineering, 9*, 383-388

Medeiros, A.S., Friel, C.E., Finkelstein, S.A., & Quinlan, R. (2012). A high resolution multi-proxy record of pronounced recent environmental change at Baker Lake, Nunavut. *Journal of Paleolimnology, 47*, 661-676

Stewardship, M.W. (2011). State of Lake Winnipeg: 1999 to 2007. In: Environment

Canada and Manitoba Water Stewardship

Tiuri, M., Sihvola, A., Nyfors, E., & Hallikaiken, M. (1984). The complex dielectric constant of snow at microwave frequencies. *IEEE Journal of oceanic Engineering, 9*, 377-382

Tjuatja, S., Fung, A.K., & Bredow, J. (1992). A scattering model for snow-covered sea ice. *IEEE Transactions on Geoscience and Remote Sensing, 30*, 804-810

WU Qihui, L.C., SUN Biao, SHI Xiaohong, ZHAO Shengnan, HAN Zhiming (2019). Change of ice phenology in the Hulun Lake from 1986 to 2017. *PROGRESS IN GEOGRAPHY, 38*, 1933-1943

WANG Jingjie LI Changyou SUN Biao FAN Cairui LIANG Lie HAN Zhiming (2017) Impacts of Precipitation on Runoff Yield of Hulun Lake Basin During 1963-2014. *Bulletin of Soil and Water Conservation*, 37(2), 115-119